

Chapter 2

Finite Temperature excitations [1]

Bose-Einstein condensation in a dilute atomic vapor [36, 54, 43] has been the subject of several experimental studies characterizing this weakly-interacting quantum fluid. In particular, measurements of interparticle interactions and the low-lying collective excitations of the condensate [91, 92, 79, 107] show excellent agreement with theoretical predictions based on a mean-field description of the condensate. This ability to make quantitative comparison between experiment and theory is one of the primary advantages of BEC in a dilute atomic gas. Previous excitation measurements were performed in a regime for which there is no detectable non-condensate fraction. This chapter expands the study of low-lying collective excitations of condensates to include higher temperatures, a regime where theoretical predictions do not yet exist. At these temperatures the interplay between condensate and non-condensate components, a potentially dissipative process not included in the usual mean-field theoretical treatment [81, 128, 59, 112, 51, 62, 66, 127, 135, 104, 67, 85, 109], strongly affects the physics. We find large energy shifts and unexpected structure in the condensate excitation spectrum, as well as a damping rate which plummets with decreasing temperature. These dramatic temperature effects have been met with interest from the theoretical community [65, 82, 103, 115, 122, 125, 126].

The apparatus and techniques used for creating a Bose-condensed sample in

a dilute atomic gas of ^{87}Rb [36, 114, 113], accurately determining its temperature [60], and probing the spectrum of low-lying collective excitations [91] are described elsewhere. We first optically trap and cool the atoms, then load them into a purely magnetic TOP (Time-averaged Orbiting Potential) trap [114]. This trap provides a cylindrically symmetric, harmonic confinement potential. Cooling the atoms in the TOP trap proceeds by forced evaporation, whereby an applied weak radio-frequency (rf) magnetic field induces Zeeman transitions to untrapped spin states [77]. The final temperature is controlled by the final frequency of the rf field. The atom cloud is observed by absorption imaging, in which the shadow of the atomic cloud is imaged onto a charge-coupled device array. To circumvent limitations of optical imaging resolution we allow the atom cloud to expand freely for 10 ms before imaging [36, 91].

The condensates are produced in a trap with radial frequency $\nu_r = 129$ Hz (365 Hz axial), with the same evaporation parameters as used in our recent quantitative study of the BEC phase transition [60]. We thus perform finite-temperature studies of condensate excitations in a well-characterized system, complementing our previous low-temperature study of collective excitations which examined the dependence on relative interaction strength. We report our results as a function of reduced temperature $T' \equiv T/T_o$, where T_o is the predicted BEC transition temperature for a harmonically confined ideal gas [7]. The estimated systematic uncertainty in T' is 5% for $T' > 0.6$, and 10% for $T' < 0.6$. At $T' < 0.6$ the non-condensate component becomes unobservably small and the temperature is inferred from the final frequency of the rf field. The lowest attainable T' is limited by the evaporation parameters and the extended size of the condensate; deeper evaporative cuts quickly reduce the number of atoms in the condensate. While plotting our results as a function of T' , we emphasize that the evaporative cooling process changes the total number of atoms as well as the temperature. Fig. 1

shows various quantities relevant for our particular evaporation parameters.

The basic spectroscopic approach for studying collective excitations follows Ref. [91]. First, a small applied sinusoidal, time-dependent perturbation to the transverse trap potential distorts the cloud. We then turn off the perturbation and the cloud freely oscillates in the unperturbed trap. Finally, the cloud is suddenly allowed to expand and the resulting cloud shape imaged. The symmetry of the drive perturbation can be varied in order to match the symmetry of a particular condensate mode. The modes are labeled by their angular momentum projection m on the trap axis. In this work, we examine the previously observed $m = 0$ and $m = 2$ modes [91, 107]. Frequency, amplitude, and damping rate of the excitations are determined as shown in Fig. 2.1. The main results of this work are shown in Fig. 2.3. For these data, the perturbative drive pulse duration was typically 14 ms, with the center frequency set to match the frequency of the excitation being studied. The response amplitudes (defined in caption for Fig. 2.2) for these data were kept small, between 5 and 15%. The radial trap frequency ν_r is calibrated by driving a $m = 1$, or “sloshing”, excitation of a cloud at $T' = 1.3$. Interatomic interactions should not affect this excitation which consists solely of rigid-body center-of-mass translation. We have also checked that anharmonicities in the confining potential are negligible in our measurements.

The normalized response frequencies as a function of T' are shown in Fig. 2.3a. Collective excitations of a non-interacting cloud should occur at twice the trap frequency (dashed line). Indeed, above the BEC phase transition, the $m = 0$ and $m = 2$ excitations are basically degenerate at $\nu/\nu_r \approx 2$. The non-condensate frequencies are consistently about 1% higher than $2\nu_r$, presumably because interactions are not completely negligible even at the relatively low densities of these clouds [8]. The non-condensate excitation frequencies do not vary significantly with temperature, even for $T' < 1$.

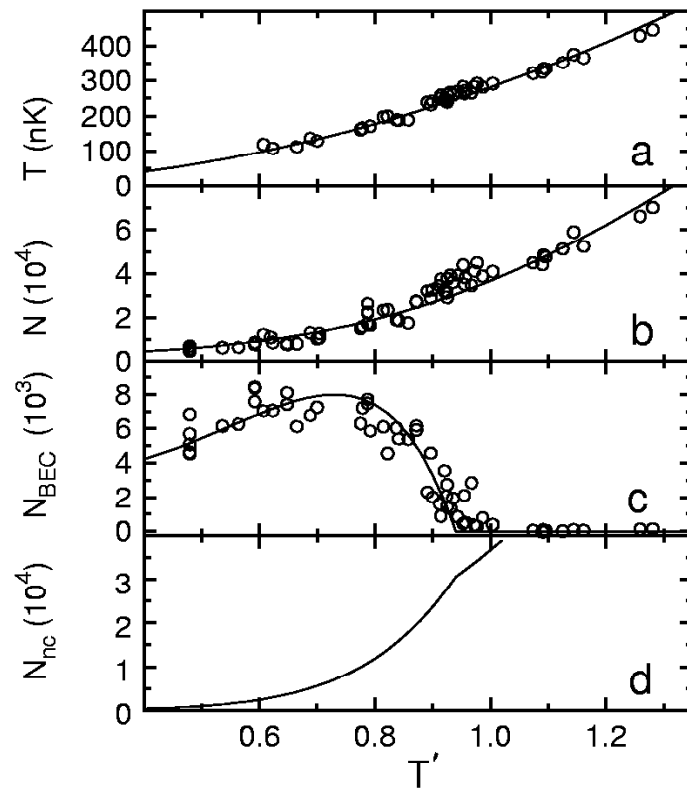


Figure 2.1: We plot temperature T (a) and total number of atoms N (b) as a function of normalized temperature T' . The relationship between N and T is not fundamental but rather a consequence of our evaporative trajectory. In (c) we plot the number of condensate atoms N_{BEC} and in (d) the inferred non-condensate number N_{nc} . Because of their different spatial extents, the peak density of the condensate component is an order of magnitude larger than that of the non-condensate component below $T' \approx 0.9$.

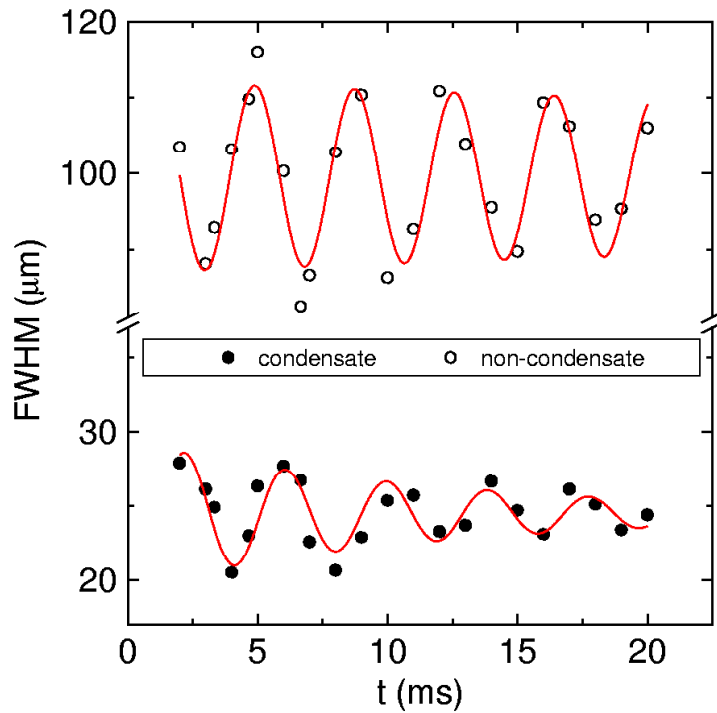


Figure 2.2: In this example, we plot the observed widths, obtained from 2-Gaussian surface fits to absorption images, of a $T' = 0.79$ cloud with an $m = 0$ excitation. The widths of each component, condensate and non-condensate, of the freely oscillating cloud are fit by an exponentially damped sine wave: $A \exp(-\gamma t) \sin(2\pi\nu t + \phi) + B$, from which we obtain the response frequency ν , initial fractional amplitude A/B , and decay rate γ . For each pair of points (condensate and non-condensate widths) a fresh cloud of atoms is cooled, excited, and allowed to evolve a time t before a single destructive measurement.

In contrast, the excitation spectrum of the condensate exhibits strong temperature dependence. While some frequency shift might be expected because of the temperature dependence of the number of condensate atoms (see Fig. 2.4), and therefore the relative interaction strength, the magnitude of the observed temperature-dependent frequency shifts is several times larger than that observed due to interaction effects [91]. In addition, the frequencies of these two modes, which are degenerate in the limit of zero interactions, actually shift in opposite directions, with only the $m = 0$ heading to the non-interacting limit. A sharp change is apparent in the slope of the temperature dependence of the $m = 0$ excitation frequency. Repeated measurements confirm that this distinct feature at $T' \approx 0.62$ reproduces. We speculate this might arise from coupling with another mode, perhaps with a strongly temperature-dependent second-sound excitation or with the excitation of the non-condensate component. No corresponding distinct feature is evident in the temperature dependence of the $m = 2$ condensate excitation frequency.

Fig. 2.3b presents the decay rate γ as a function of temperature. While the frequencies of the two condensate modes behave very differently, their decay rates appear to fall on a single curve, with γ quickly decreasing with decreasing T' [9]. Another remarkable feature is that for temperatures where two-component clouds are observed, the condensate excitations damp much faster than their non-condensate counterparts (see also Fig. 2.2). The strong temperature dependence suggests that finite decay times reported in Refs. [91] and [107] were due to the finite temperature of the samples and that condensate excitations may persist for very long times at lower T' .

In the limit of low amplitude response, the measured spectrum corresponds to the elementary excitations of BEC in a dilute gas. At our lowest temperature, $T' \approx 0.48$, we examine the condensate excitations as a function of increasing

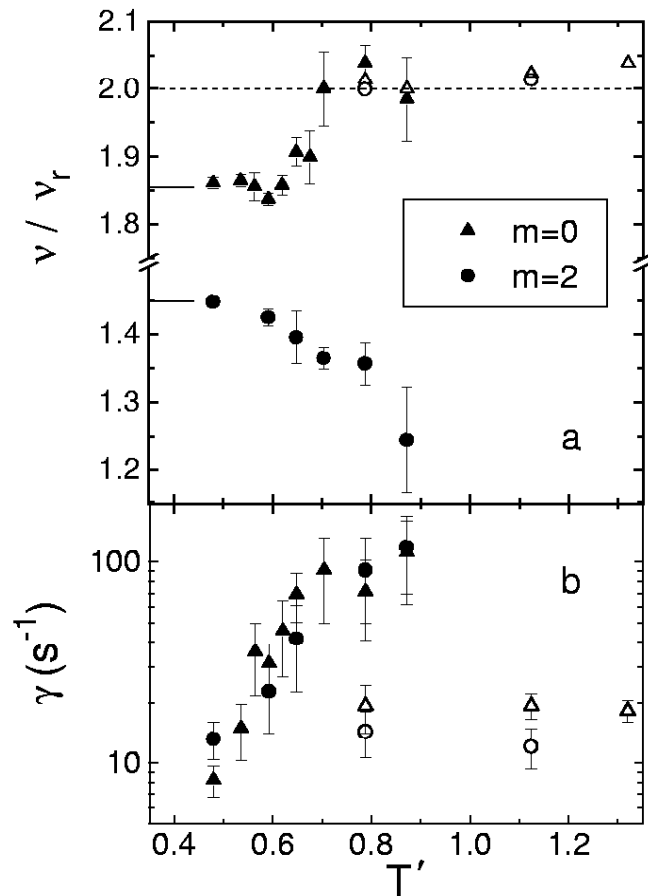


Figure 2.3: Temperature-dependent excitation spectrum: (a) Frequencies (normalized by the radial trap frequency) for $m = 0$ (triangles) and $m = 2$ (circles) collective excitation symmetries are shown as a function of normalized temperature T' . Oscillations of both the condensate (solid symbols) and non-condensate (open symbols) clouds are observed. Short lines extending from the left side of the plot mark the mean-field theoretical predictions in the $T = 0$ limit (for 6000 atoms in our trap) [8]. (b) For both the $m = 0$ and $m = 2$ condensate excitations the damping rate γ quickly decreases with decreasing temperature.

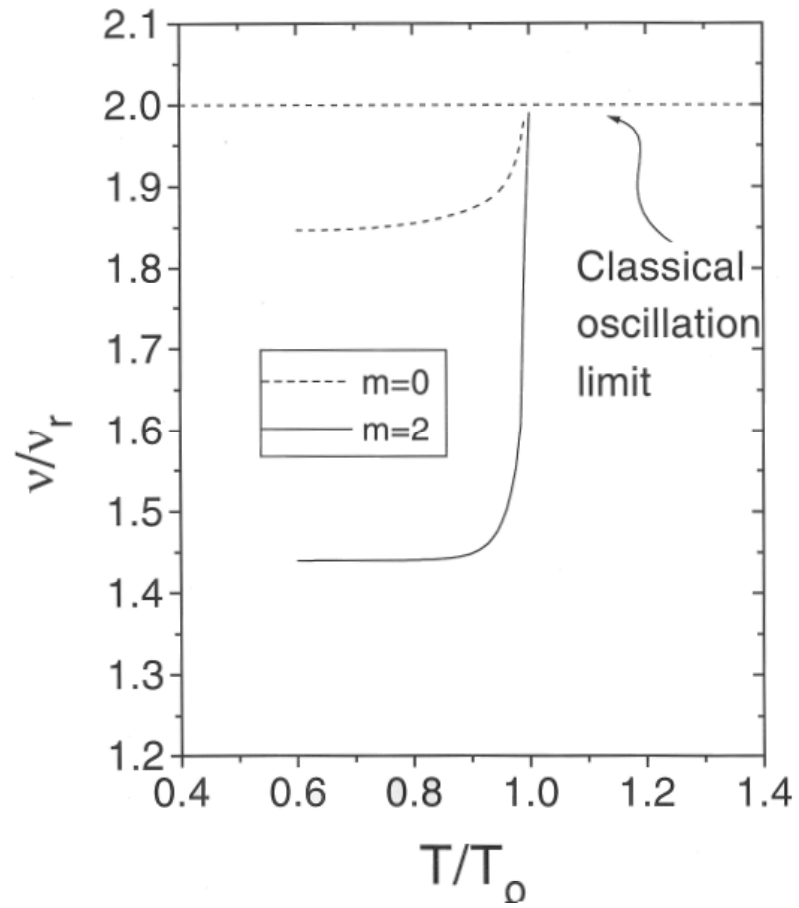


Figure 2.4: A simple model based on the theory by Edwards [59], which only takes into account the change in mean field due to the changing number of atoms in the condensate as a function of temperature.

response amplitude. The $m = 0$ mode exhibits a significantly smaller anharmonic frequency shift than the mode with $m = 2$ symmetry (Fig. 2.5a). The decay rates γ for the $m = 0$ and $m = 2$ condensate excitations show some dependence on response amplitude (Fig. 2.5b), but in neither case does γ approach zero in the limit of small response. These data demonstrate that ν and γ measured for a typical response amplitude of 10% are fairly close to the zero-amplitude perturbation limit.

For comparison with the results of our free-evolution spectroscopy technique, Fig. 2.6 presents a more conventional resonance measurement. While the central frequency is in good agreement with that measured from observing the freely oscillating widths as discussed above, the resonance technique is inefficient in terms of data collection time and moreover vulnerable to systematic errors, particularly when one tries to extract a damping rate from the linewidth.

This experiment extends previous studies of condensate excitations to temperatures for which both condensate and non-condensate atoms are present in significant numbers. This regime is not yet well understood theoretically, as the standard mean-field theoretical treatment of collective excitations of a harmonically confined dilute BEC is done for the $T = 0$ limit and does not include dissipation. Both $m = 0$ and $m = 2$ condensate modes exhibit large temperature-dependent frequency shifts. The decay rate of the condensate collective excitations decreases rapidly with temperature, and shows no signs of leveling off. More recently, there have been further theoretical investigations into finite temperature modes [56, 73, 110].

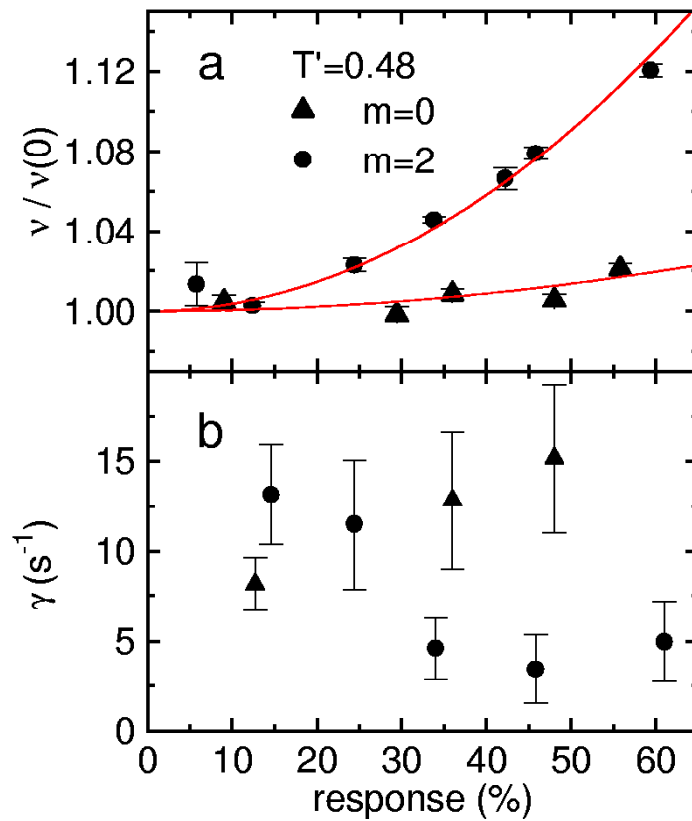


Figure 2.5: For large response amplitudes at our lowest temperature, $T' \approx 0.48$, we measure the shift in the response frequency ν and damping rate γ . In (a) the frequencies, normalized by the small drive limit, show a larger anharmonic shift for the $m = 2$ condensate excitation than for the $m = 0$ case. (Some of the $m = 2$ data is the same as presented in Ref. 4 and is reproduced here to facilitate comparison.) Solid lines are guides to the eye. In (b) the decay rates γ for the $m = 0$ and $m = 2$ condensate modes shift in opposite directions with increasing response amplitude.

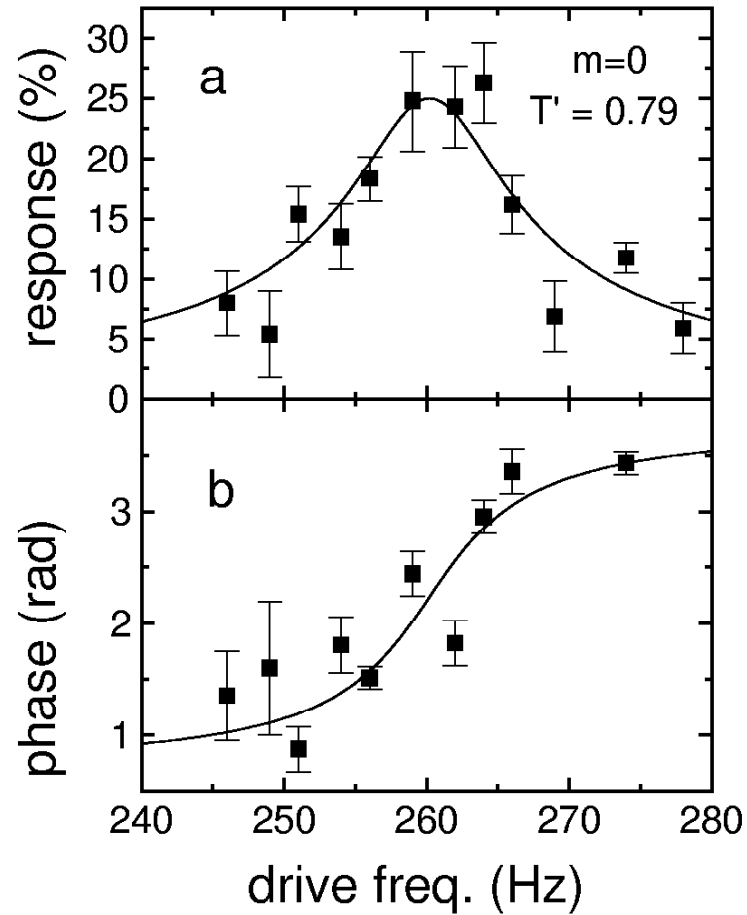


Figure 2.6: The response of the $m = 0$ condensate excitation at $T' = 0.79$ as a function of the center drive frequency. Solid lines show fits to the expected form for the amplitude (a) and phase (b) of a driven harmonic oscillator in the presence of damping. For these measurements a constant amplitude drive is applied with a duration of 150 ms (about 7 Hz FWHM in frequency), after which the resulting excitation is observed for 10 ms to determine amplitude and phase.